

Free space optical system performance for laser beam propagation through non-Kolmogorov turbulence

Original

Free space optical system performance for laser beam propagation through non-Kolmogorov turbulence / Italo, Toselli; LARRY C., Andrews; RONALD L., Phillips; Ferrero, Valter. - 6457:(2007), pp. 64570T-1-64570T-11. (Intervento presentato al convegno SPIE: Free-Space Laser Communication Technologies XIX and Atmospheric Propagation tenutosi a San Josè, California nel January 24 th, 2007) [10.1117/12.698707].

Availability:

This version is available at: 11583/1995694 since: 2016-11-04T15:00:16Z

Publisher:

Published

DOI:10.1117/12.698707

Terms of use:

This article is made available under terms and conditions as specified in the corresponding bibliographic description in the repository

Publisher copyright

(Article begins on next page)

Free space optical system performance for laser beam propagation through non Kolmogorov turbulence

Italo Toselli^a, Larry. C. Andrews^b, Ronald L. Phillips^c, Valter Ferrero^a

^aOptical Communications Group, Politecnico di Torino, 10128 Turin, Italy

^bDepartment of Mathematics, University of Central Florida, Orlando, FL32816

^cUniversity of Central Florida, Florida Space Institute, MS: FSI, Kennedy Space Center, FL 32899

ABSTRACT

Free space laser system performance is limited by atmospheric turbulence that has been described for many years by Kolmogorov's power spectral density model because of its simplicity. Unfortunately several experiments have been reported recently that show Kolmogorov theory is sometimes incomplete to describe atmospheric statistics properly, in particular in portions of the troposphere and stratosphere. In this paper we present a Non-Kolmogorov power spectrum which uses a generalized exponent instead of constant standard exponent value $11/3$ and a generalized amplitude factor instead of constant value 0.033 . Using this new spectrum in weak turbulence, we carry out, for horizontal path, analysis of Long Term Beam Spread, Scintillation index, Probability of fade, mean SNR and mean BER as variation of the spectrum exponent.

Keywords: Atmospheric turbulence, structure function, Kolmogorov spectrum, beam spread, scintillation, fade, SNR, BER .

1. INTRODUCTION

For a long time, the structure function has been modeled according to Kolmogorov's power spectrum of refractive index fluctuations which is widely accepted and has been applied extensively in studies of optical and radio wave propagation in the atmosphere. However, recent experimental data from space-based stellar scintillation, balloon-borne in-situ temperature, and ground-based radar measurements indicate turbulence in the upper troposphere and stratosphere deviates from predictions of the Kolmogorov model [5][9][10]. Further development of the turbulent theory of passive scalar transfer has shown that although the Kolmogorov spectrum is important, it constitutes only one part of the more general behavior of passive scalar transfer in a turbulent flow [6]. Some anomaly behavior [3] seems to occur when the atmosphere is extremely stable because under such condition the turbulence is no longer homogeneous in three dimensions since the vertical component is suppressed. It has been shown [4] that for such two dimensional turbulence, coherent vortices can develop that reduce the rate of the energy cascade from larger to smaller scales. As a result Kolmogorov turbulence will not develop. In addition anisotropy in stratospheric turbulent inhomogeneities has been experimentally investigated [5][8][11][12]. We must accept de facto that turbulence is still an unsolved problem in classical physics and scientists community must persist in doing more simulations, measurements and experiments [7]. It is very important, therefore, to find new models more general than Kolmogorov spectrum in order to describe experimental data also in non Kolmogorov turbulence. In this paper we present a theoretical spectrum model which reduces to one of Kolmogorov only for a particular case of its exponent: the standard value $11/3$. Exponent can assume all the values between the range 3 to 4. Using this new spectrum, following the same procedure already used from Andrews and Phillips [1][2], we have analyzed the impact of the exponent's variation on *Long Term Beam Spread*, *Scintillation index*, *Probability of fade*, *mean Signal to Noise Ratio (SNR)* and *mean Bit Error Rate (BER)* for horizontal path, that is for constant value of the refractive index structure parameter.

2. NON KOLMOGOROV SPECTRUM

The basic power-law spectrum of Kolmogorov is defined by

$$\Phi_n(\kappa) = 0.033 \cdot C_n^2 \cdot \kappa^{-11/3} \quad (1)$$

where C_n^2 is the refractive-index structure parameter. The validity of the Kolmogorov spectrum is restricted to the inertial range although in some analyses it is extended to all spatial wave numbers. Here we examine a more general power spectrum model that describes non-Kolmogorov atmospheric turbulence in which the power law exponent 11/3 is allowed to deviate somewhat from this value.

We assume that in an atmosphere exhibiting non-Kolmogorov turbulence the structure function for the index of refraction is given by

$$D_n(r) = \beta \cdot C_n^2 \cdot r^\gamma \quad (2)$$

where γ is the power law which reduces to 2/3 in the case of conventional Kolmogorov turbulence. Here, β is a constant equal to unity when $\gamma = 2/3$, but otherwise has units $\text{m}^{-\gamma+2/3}$. Following same procedure reported in [1], the corresponding power-law spectrum associated with structure function takes the form

$$\Phi_n(\kappa, \alpha) = A(\alpha) \cdot \tilde{C}_n^2 \cdot \kappa^{-\alpha}, \quad \kappa > 0, \quad 3 < \alpha < 4, \quad (3)$$

where $\alpha = \gamma + 3$ is the spectral index or power law, $\tilde{C}_n^2 = \beta \cdot C_n^2$ is a generalized structure parameter with units $\text{m}^{-\gamma}$, and $A(\alpha)$ is defined by

$$A(\alpha) = \frac{1}{4\pi^2} \Gamma(\alpha - 1) \cos\left(\frac{\alpha\pi}{2}\right), \quad 3 < \alpha < 4 \quad (4)$$

and the symbol $\Gamma(x)$ in the last expression is the gamma function. When $\alpha = 11/3$, we find that $A(11/3) = 0.033$ and the generalized power spectrum reduces to the conventional Kolmogorov spectrum. Also, when the power law approaches the limiting value $\alpha = 3$, the function $A(\alpha)$ approaches zero. Consequently, the refractive-index power spectral density vanishes in this limiting case.

3. LONG TERM BEAM SPREAD

The first important quantity that shows total average beam spot size radius on the receiver lens is the Long Term Beam Spread. It can be written as the sum of three terms: diffraction limited beam spreading, beam spreading due to small turbulence scales and beam wander which can be described by the variance of the instantaneous center of the beam in the receiver plane.

The analytical form of *Long Term Beam Spread* for a Gaussian beam wave is [1]

$$W_e^2 = \langle W_{LT}^2(\alpha) \rangle = W^2 \cdot [1 + \langle T(\alpha) \rangle] \quad (5)$$

where W is the diffraction limited spot size radius and $\langle T(\alpha) \rangle$ is the term which includes small scale beam spreading and beam wander atmospheric effects.

In order to carry out Long Term Beam Spread analysis we need to calculate the $\langle T(\alpha) \rangle$ term.

For horizontal path the parameter C_n^2 that appears inside the relation $\tilde{C}_n^2 = \beta \cdot C_n^2$ is constant. Following same formula reported in [1] but using the Non Kolmogorov spectrum (3), we carry out

$$T(\alpha) = 4\pi^2 k^2 L \cdot \left(\int_0^1 \int_0^\infty \kappa \cdot \phi_n(\alpha, \kappa) d\kappa d\xi - \int_0^1 \int_0^\infty \kappa \cdot \phi_n(\alpha, \kappa) \exp\left(-\frac{\Lambda L \kappa^2 \xi^2}{k}\right) d\kappa d\xi \right) \quad (6)$$

$$= -16 \cdot A(\alpha) \cdot \frac{1}{\alpha-1} \cdot \Gamma\left(1-\frac{\alpha}{2}\right) \cdot \Lambda^{\frac{\alpha-1}{2}} \cdot \tilde{\sigma}_R^2(\alpha)$$

where $\xi = 1 - \frac{z}{L}$ (z is the propagation distance), $\Lambda = \frac{2L}{kW^2}$ and we have defined a Non Kolmogorov Rytov variance

$$\tilde{\sigma}_R^2(\alpha) = 1.23 \cdot \tilde{C}_n^2 \cdot k^{3-\frac{\alpha}{2}} \cdot L^{\frac{\alpha}{2}} \quad (7)$$

It is interesting to observe that for $\alpha = 11/3$ we obtain the particular case of the Kolmogorov spectrum already reported in [1].

At this point, we plot in figure 1 the *long term beam spread* for a particular case, taking:

$$L = 1\text{km}; \tilde{C}_n^2 = 7 \cdot 10^{-14} m^{-\alpha+3}; \lambda = 1.55 \mu\text{m}; W_0 = 0.01\text{m}.$$

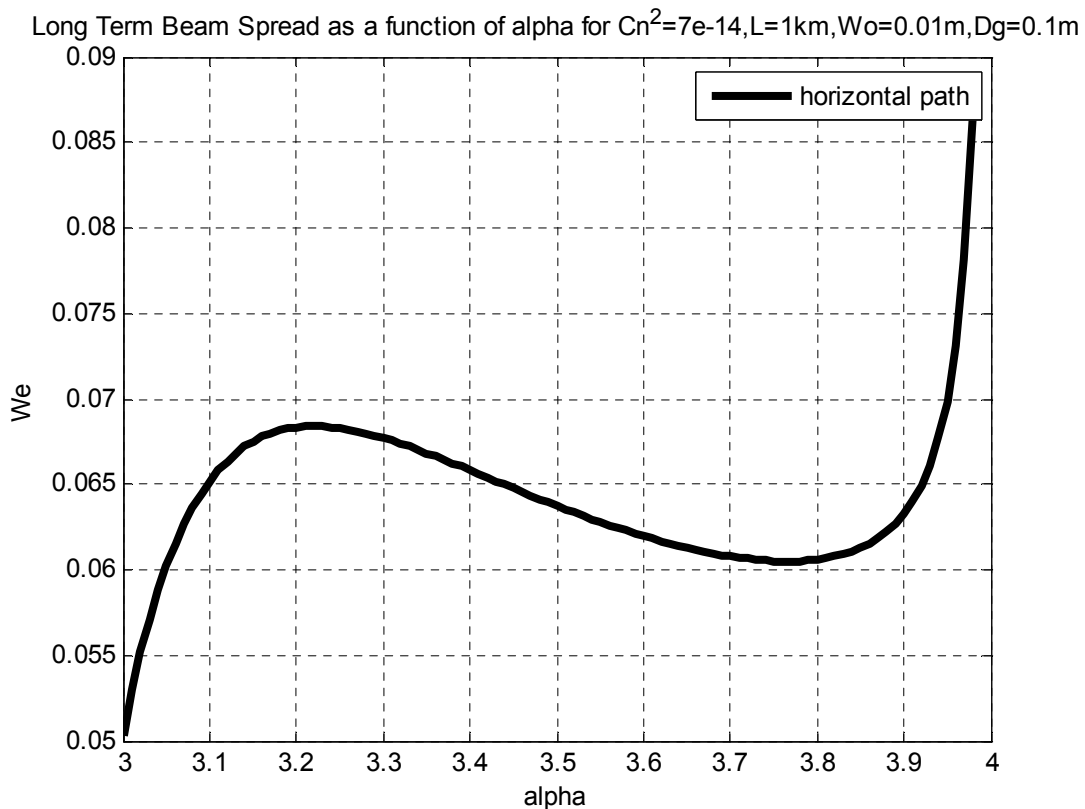


Figure 1- Long Term Beam Spread as a function of alpha for horizontal path

We deduce from figure 1 that if alpha decreases from $\alpha = 11/3$ than *long term beam spread* W_e increases up to a maximum value. At this point the curve changes its slope because of the term $A(\alpha)$ that assumes very low values. In addition it is shown that if alpha increases from $\alpha = 11/3$ than *long term beam spread* W_e decreases up to a minimum value. At this point the curve changes its slope because of the term $\Gamma\left(1 - \frac{\alpha}{2}\right)$ that assumes high values close to its asymptote.

4. SCINTILLATION INDEX

Another important parameter that is necessary in order to calculate the system performance is the scintillation index. In our analysis we include aperture averaging effects of the receiver aperture, so we carry out the flux variance in the plane of the detector of diameter D_G . We presume very similar results with respect to Gaussian scintillation index [1]. Finally, in our analysis we assume that beam wander induced scintillation is negligible which is true when we consider either a plane wave or a spherical wave, but the situation is different for focused beams [1].

4.1 Horizontal path: plane wave model and spherical wave model

Following the same procedure as discussed in [1] for the standard Kolmogorov spectrum, but this time using a Non-Kolmogorov spectrum and introducing receiver diameter D_G , our analysis for plane wave model leads to

$$\begin{aligned} \sigma_{I_plane}^2(\alpha, D_G) &= 8\pi^2 \cdot k^2 \cdot L \cdot \text{Re} \left\{ \int_0^1 \int_0^\infty \kappa \cdot \Phi_n(\kappa, \alpha) \cdot \exp\left(-\frac{D_G^2 \cdot \kappa^2}{16}\right) \cdot \left[1 - \exp\left(-j \frac{L \cdot \kappa^2 \cdot \xi}{k}\right)\right] d\kappa d\xi \right\} \\ &= 6.5 \cdot \pi^2 \cdot A(\alpha) \cdot \tilde{\sigma}_k^2(\alpha) \cdot \Gamma\left(1 - \frac{\alpha}{2}\right) \cdot \frac{1}{\alpha} \cdot \left\{ \frac{\alpha}{2} \cdot \left(\frac{k \cdot D_G^2}{16 \cdot L}\right)^{\frac{\alpha}{2}-1} - \left[\left(\frac{k \cdot D_G^2}{16 \cdot L}\right)^2 + 1 \right]^{\frac{\alpha}{4}} \cdot \sin\left[\frac{\alpha}{2} \cdot \text{arctg}\left(\frac{16 \cdot L}{k \cdot D_G^2}\right)\right] \right\} \end{aligned} \quad (8)$$

Also in this case it is interesting to observe that for $\alpha = 11/3$ we have a particular case of Kolmogorov spectrum already reported in [1].

Our analysis for spherical wave model leads to

$$\begin{aligned} \sigma_{I_spherical}^2(\alpha, D_G) &= 8\pi^2 \cdot k^2 \cdot L \cdot \text{Re} \left\{ \int_0^1 \int_0^\infty \kappa \cdot \Phi_n(\kappa, \alpha) \cdot \exp\left(-\frac{D_G^2 \cdot \kappa^2 \cdot \xi^2}{16}\right) \cdot \left[1 - \exp\left(-j \frac{L \cdot \kappa^2 \cdot \xi \cdot (1-\xi)}{k}\right)\right] d\kappa d\xi \right\} \\ &= 4\pi^2 \cdot k^2 \cdot L \cdot A(\alpha) \cdot \tilde{C}_n^2 \cdot \left(\frac{16}{D_G^2}\right)^{1-\frac{\alpha}{2}} \cdot \Gamma\left(1 - \frac{\alpha}{2}\right) \cdot \left\{ \frac{1}{\alpha-1} - \text{Re} \left\{ \int_0^1 \left(\xi^2 + j \frac{16 \cdot L \cdot \xi \cdot (1-\xi)}{k \cdot D_G^2} \right)^{\frac{\alpha}{2}-1} d\xi \right\} \right\} \end{aligned} \quad (9)$$

At this point, we can plot both $\sigma_{I_plane}^2(D_G)$ and $\sigma_{I_spherical}^2(D_G)$ as a function of alpha for a particular horizontal case. We take

$$L = 1km; \tilde{C}_n^2 = 7 \cdot 10^{-14} m^{-\alpha+3}; \lambda = 1.55\mu m; D_G = 0.1m.$$

The results are shown in figure 2.

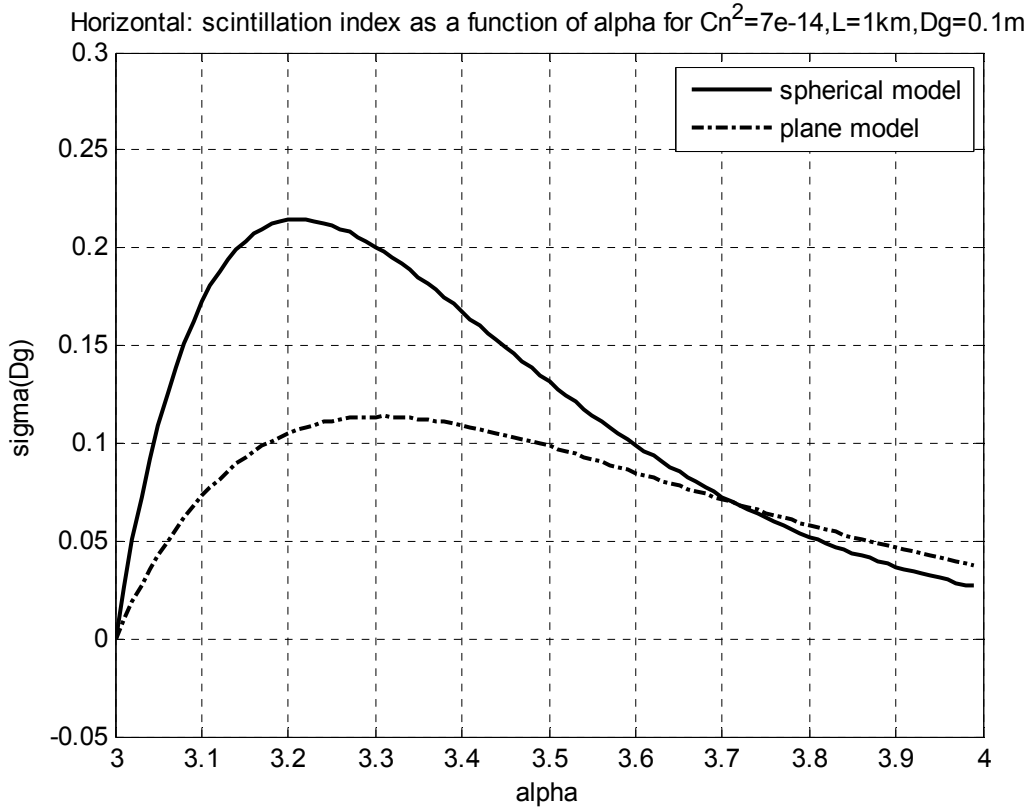


Figure 2 -Scintillation index as a function of alpha for horizontal path using spherical wave model and plane wave model

We deduce from figure 2 that for alpha values lower than Kolmogorov value $\alpha = 11/3$, there is an increase of scintillation both for spherical model and plane model, but for spherical model it is more remarkable. It will be shown subsequently that an increase of scintillation leads to a penalty on the system performance. We deduce also that there are two maximum values of scintillation respectively for alpha values close to 3.3 for plane model and close to 3.2 for spherical model. At these points the curves change their slopes because of the term $A(\alpha)$ that assumes very low values and scintillation begins to decrease up to zero. In addition for alpha values higher than $\alpha = 11/3$, scintillation slightly decreases for both the wave model and spherical model and consequently it leads to a slight gain on the system performance.

5 PROBABILITY OF FADE

Given a PDF model for irradiance fluctuations $p_I(I)$, the probability of fade describes the percentage of time the irradiance of the received signal is below some prescribed threshold value I_T . Hence, the probability of fade as a function of threshold level is defined by the cumulative probability [1]

$$p_I(I < I_T) = \int_0^{I_T} p_I(I) dI \quad (10)$$

The PDF most often used under weak irradiance fluctuations is the lognormal model and the resulting probability of fade leads to

$$p_I(I < I_T) = \frac{1}{2} \cdot \left\{ 1 + \operatorname{erf} \left[\frac{\frac{1}{2} \cdot \sigma_I^2(\alpha, D_G) - 0.23 \cdot F_T}{\sqrt{2} \cdot \sigma_I(\alpha, D_G)} \right] \right\}, \quad (11)$$

where $\operatorname{erf}(x)$ is the error function. In arriving at this expression we have introduced the fade threshold parameter

$$F_T = 10 \cdot \log_{10} \left(\frac{\langle I \rangle}{I_T} \right) [dB] \quad (12)$$

The fade parameter F_T , given in decibels [dB], represents the dB level below the on-axis mean irradiance that the threshold I_T is set.

5.1 Horizontal link: plane wave model and spherical wave model

Using scintillation index for plane wave model (8) and for spherical wave model (9) into equation (11), we calculate the *Probability of Fade* as a function of alpha for a fixed fade threshold parameter for a particular horizontal case.

We take

$$L = 1km; \tilde{C}_n^2 = 7 \cdot 10^{-14} m^{-\alpha+3}; \lambda = 1.55 \mu m; D_G = 0.1m, F_T = 6dB$$

The plot is shown in figure 3 where are reported both plane wave model and spherical wave model.

It is clear now that alpha variation has impact on the fade probability for both spherical and plane wave models, in particular lower alpha values lead to a penalty on the fade performance. In addition we can observe that the spherical model predicts higher probability of fade than plane wave model for alpha values lower than alpha value intersection point (around $\alpha = 3.72$); for alpha values higher than alpha value intersection point the situation is opposite. Also for this diagram there is a maximum point where the curves change their slope because of the scintillation that begins to decrease up to zero.

Under the same conditions we plot the Probability of Fade as a function of fade threshold parameter for several alpha values. Both plane wave and spherical wave cases are illustrated respectively in figure 4 and figure 5.

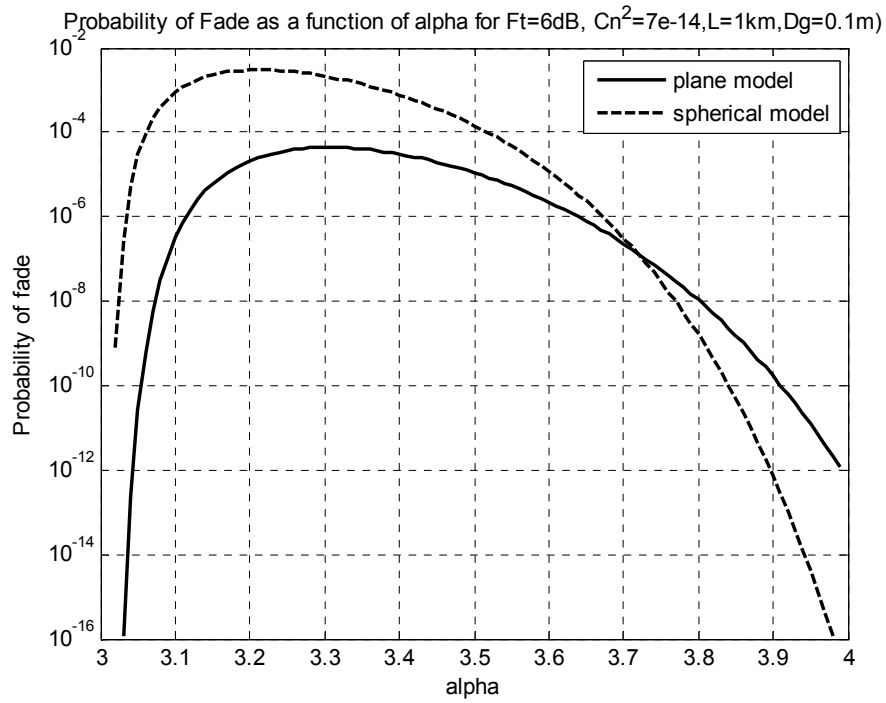


Figure 3 – Probability of fade as a function of alpha using the log-normal PDF and two different models for the scintillation index: plane wave model and spherical wave model

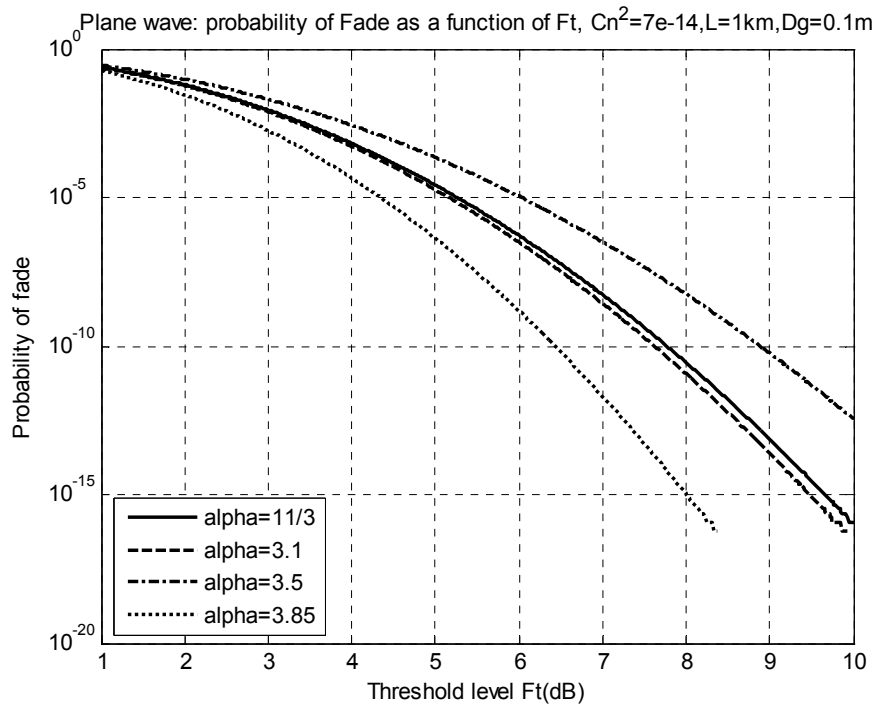


Figure 4 – Probability of fade as a function of Threshold level for several values of alpha using plane wave scintillation index.

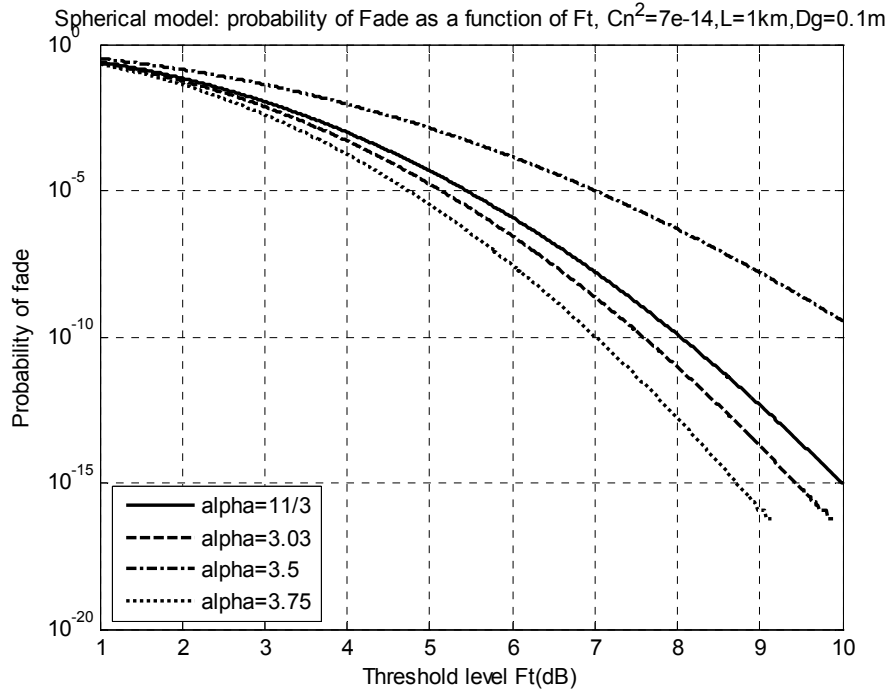


Figure 5 – Probability of fade as a function of Threshold level for several values of alpha using spherical wave scintillation index.

6. MEAN SIGNAL TO NOISE RATIO

In this paragraph is shown the *Mean Signal to Noise Ratio* in presence of atmospheric turbulence using Non Kolmogorov power spectrum. The received irradiance over long measurement intervals must be treated like random variable because of the turbulence. Based on [1][2], the mean Signal to Noise Ratio $\langle SNR \rangle$ at the output of the detector in the case of a shot-noise limited system assumes the form

$$\langle SNR \rangle = \frac{SNR_0}{\sqrt{1 + \sigma_I^2(\alpha, D_G) \cdot SNR_0^2}} \quad (13)$$

where $\sigma_I^2(\alpha, D_G)$ has been defined before, SNR_0 is the signal to noise ratio in absence of turbulence.

6.1 Horizontal link: plane wave model

We plot in dB units Mean Signal to Noise Ratio $\langle SNR \rangle$ as a function of Signal to Noise Ratio without turbulence SNR_0 for several alpha values, using plane wave model for scintillation. We take follow parameters

$$L = 1km; \tilde{C}_n^2 = 7 \cdot 10^{-14} m^{-\alpha+3}; \lambda = 1.55\mu m; D_G = 0.1m.$$

The plot is shown in figure 6. It is shown the impact of the alpha variation on the $\langle SNR \rangle$ performance. Again, when alpha is lower than $\alpha = 11/3$ there is a translation of the curves toward the bottom or in other words there is a penalty on the system performance. From another side for alpha value higher than $\alpha = 11/3$ there is a gain on the system performance with respect to the case of Kolmogorov $\alpha = 11/3$. Finally also there is a gain on system performance with respect to Kolmogorov $\alpha = 11/3$ when alpha assumes values very close to $\alpha = 3$ because of the amplitude

factor $A(\alpha)$ that assumes very low values and consequently the *scintillation* reported before in figure 2 approaches to zero.

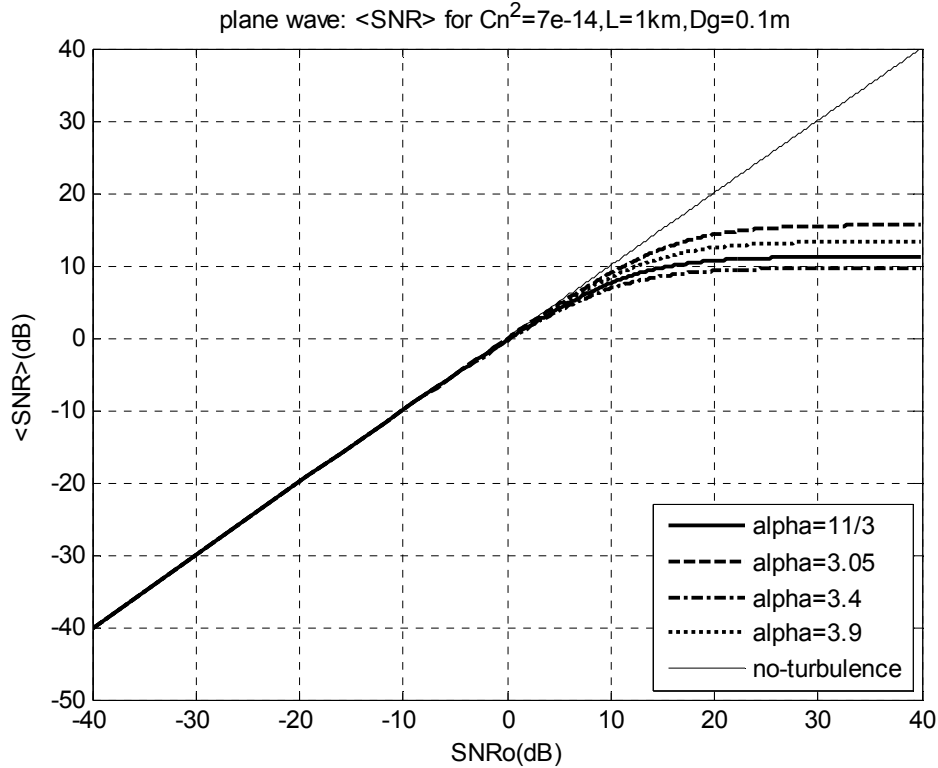


Figure 6 - Mean Signal to Noise Ratio as a function of Signal to Noise Ratio without turbulence for several alpha values, using plane wave model for scintillation.

7. MEAN BIT ERROR RATE

In the presence of optical turbulence, the probability of error is considered a conditional probability that must be averaged over the PDF of the random signal to determine the unconditional mean BER. In terms of a normalized signal with unit mean, this leads to the expression [1] [2]

$$\Pr(E) = \langle BER \rangle = \frac{1}{2} \cdot \int_0^{\infty} p_I(u) \cdot \operatorname{erfc}\left(\frac{\langle SNR \rangle \cdot u}{2 \cdot \sqrt{2}}\right) du, \tag{14}$$

where $p_I(u)$ is taken log normal distribution with unit mean

$$p_I(u) = \frac{1}{u \cdot \sigma_I(D_G, \alpha) \cdot \sqrt{2 \cdot \pi}} \cdot \exp\left\{-\frac{\left[\ln(u) + \frac{1}{2} \cdot \sigma_I^2(D_G, \alpha)\right]^2}{2 \cdot \sigma_I^2(D_G, \alpha)}\right\}, u > 0 \tag{15}$$

We plot the *Mean Bit Error Rate* as a function of the $\langle SNR \rangle$ for several alpha values.

7.1 Horizontal link: plane wave model

We plot the Mean Bit Error Rate as a function of $\langle SNR \rangle$ for several alpha values using plane wave model for scintillation. We take same parameters

$$L = 1km; \tilde{C}_n^2 = 7 \cdot 10^{-14} m^{-\alpha+3}; \lambda = 1.55 \mu m; D_G = 0.1m.$$

The plot is shown in figure 7

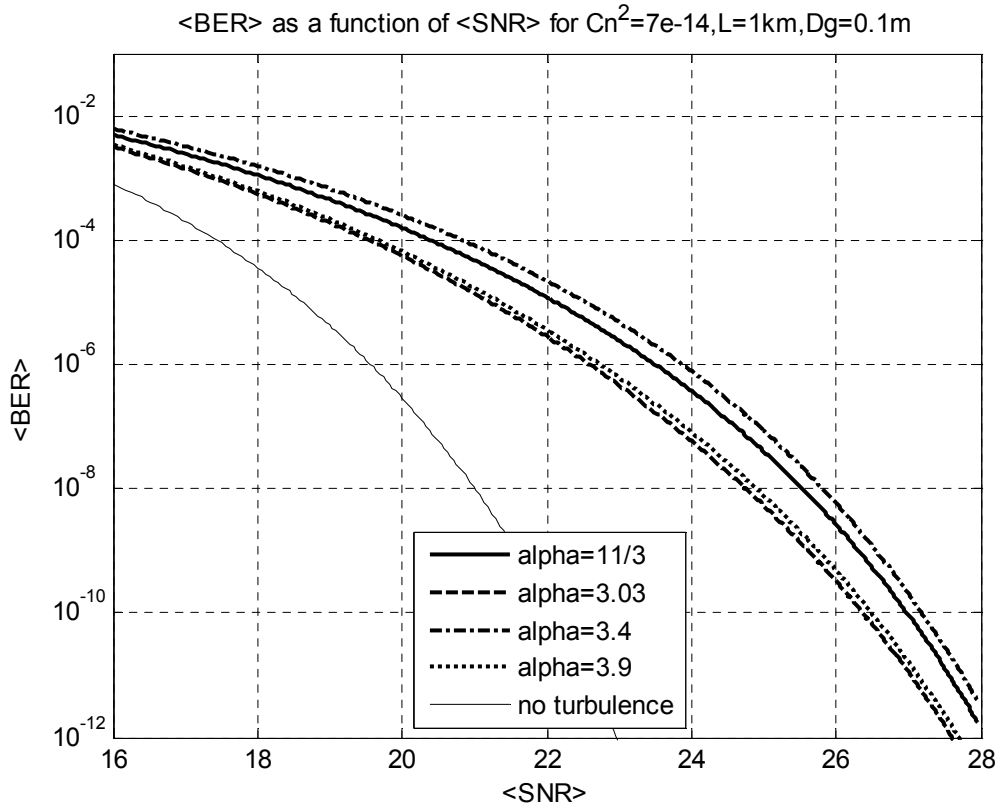


Figure 7 - Mean Bit Error Rate as a function of Mean Signal to Noise Ratio for several alpha values, using plane wave model for scintillation.

It is shown the impact of the alpha variation on $\langle BER \rangle$ performance. Also in this analysis when alpha is lower than $\alpha = 11/3$ there is a penalty, but for alpha higher than $\alpha = 11/3$ there is a improvement on the system performance.

However when alpha assumes values close to $\alpha = 3$ there is a gain on the $\langle BER \rangle$ performance with respect to $\langle BER \rangle$ value correspondent to $\alpha = 11/3$ because of the scintillation approaches to zero.

8. DISCUSSION

It has been introduced a Non-Kolmogorov power spectrum which uses both a generalized exponent and a generalized amplitude factor instead of a constant standard exponent value $\alpha = 11/3$ and of a constant amplitude factor 0.033 such is for Kolmogorov spectrum. This Non-Kolmogorov spectrum has been carried out from a generalized structure function. It has been shown, for horizontal link, *Long Term Beam Spread, Scintillation, Probability of fade, mean SNR*

and *mean BER* as variation of alpha exponent that assumes values around the standard value of Kolmogorov $\alpha = 11/3$.

For horizontal links, it has been shown that for lower alpha values than $\alpha = 11/3$, but not for alpha close to $\alpha = 3$, there is a remarkable increase of scintillation and consequently a major penalty on the system performance. However when alpha assumes value close to $\alpha = 3$ the amplitude factor $A(\alpha)$ assumes very low value and consequently *Long Term Beam Spread* and *Scintillation* decrease leading an improvement on the system performance. Finally also for higher alpha values than $\alpha = 11/3$ *Scintillation* decreases and consequently it improves the system performance.

8. REFERENCES

1. Larry C. Andrews, Ronald L. Phillips. *Laser Beam Propagation through Random Media*. Spie Press, second edition - 2005.
2. Larry C. Andrews, Ronald L. Phillips, Cynthia Y. Hopen. *Laser Beam Scintillation with Applications*. Spie Press, 2001.
3. David Dayton, Bob Pierson, Brian Spielbusch. *Atmospheric structure function measurements with a Shack-Hartmann wave front sensor*. Optics letters ,vol.17, num. 24,1992.
4. J. McWilliam, Phys. Fluids, A 2, 547, 1990
5. Mikhail S. Belenkii, Stephen J. Karis, James M. Brown II, and Robert Q. Fugate. *Experimental study of the effect of non-Kolmogorov stratospheric turbulence on star image motion*. SPIE vol. 3126.
6. Ephim Golbraikh, Norman S. Kopeika. *Behavior of structure function of refraction coefficients in different turbulent fields*. Applied Optics, vol 43, num. 33, 2004.
7. Gregory Falkovich, Katepalli R. Sreenivasan. *Lessons from Hydrodynamic Turbulence*. Physics Today, April 2006.
8. A I Kon. *Qualitative theory of amplitude and phase fluctuations in a medium with anisotropic turbulent irregularities*. Wave in random media 4, 297-305, 1994.
9. Bruce E. Stribling, Byron M. Welsh and Michael C. Roggemann. *Optical propagation in Non-Kolmogorov Atmospheric Turbulence*. SPIE vol.2471, 181-196.
10. Demos T. Kyrakis, John Wissler, Donna D.B. Keating, Amanda J.Preble, Kenneth P. Bishop. *Measurement of optical turbulence in the upper troposphere and lower stratosphere*. SPIE vol. 2110, 1994.
11. Mikhail S. Belen'kii, Stephen J.Karis, Christian L. Osmon. *Experimental evidence of the effects of non-Kolmogorov turbulence and anisotropy of turbulence*. SPIE vol. 3749, 1999.
12. Robert R. Beland, *Some aspects of propagation through weak isotropic non-Kolmogorov turbulence*. SPIE vol. 2375